Crack-Based Complementary Nanoelectromechanical Switches for Reconfigurable Computing

Qiang Luo, Zhe Guo, Shuai Zhang, Xiaofei Yang, Xuecheng Zou, Jeongmin Hong, and Long You, *Member, IEEE*

***Abstract*— Reconfigurable computing (RC) enables hardware to operatewith the flexibility of software. This is achieved by programming the interconnections between logic blocks. In this study,we exploited crack-based complementary nanoelectromechanical (CNEM) switches to construct energy-efficient and high-density RC. Our proposed device integrates the advantages of ferroelectric and NEM switch, such as nonvolatility, a quasi-zero OFF-state leakage current and a low operating voltage. Complementary switching enables our device to operate asa CMOS inverter in a very simple manner. Thus, this device can readily implement programmable routings. The voltage required to maintain the routings is not needed, leading to significant saving in static and dynamic power consumption. In addition, the fundamental AND, OR and NOT logic gates can be condensed into a single CNEM switch device to implementthe reconfigurable logics, thereby reducing chip area and energy dissipation. We believe that our device paves the way for development of energy-efficient electronics.**

***Index Terms*— CNEM switches, electric field control, switchable cracks, reconfigurable computing.**

I. Introduction

RECONFIGURABLE computing (RC) can be specialized to a particular task through its universal programmability, offering large flexibility and short time from design to realization [1]–[3]. Yet, conventionally, RC based on CMOS technology often consumes high static and dynamic power consumption [4]. Further decrease of leakage current, even to zero, and operating voltage was bounded [5], [6]. In addition, the requirement of voltages to maintain the data and routing paths in RC introduces additional power dissipation [7]. Moreover, with further dimensional scaling, a remarkable growth of energy dissipation will take place [8]. Therefore, considerable effort has been devoted to beyond-CMOS devices that can exhibit nonvolatility, simplicity, and energy efficiency, such as spintronics [9], ferroelectric [10] and nanoelectromechanical (NEM) switches [11], [12].

Ferroelectric devices, which generally exploits ferroelectric polarization switching, feature nonvolatility, high speed and low energy, but a non-destructive readout process is highly desirable [13]. NEM switches, which constitute another type of beyond-CMOS devices, created exciting opportunities for energy-efficient electronic devices owing to the quasi-zero OFF-state leakage current and abrupt switching behavior [14], [15]. Electrostatically actuated NEM switches usually rely on a cantilever or suspended nanostructure, which is implemented through an involved fabrication process. A complementary structure is even more difficult [16], [17].

Recently, a single-crack based NEM switch that combines the advantages of both ferroelectric and NEM switches was demonstrated for memory applications [18], [19]. Such cracks are originally induced from ferroelectric oxide. The naturally formed nanoscale air gap enables its behave as a NEM switch. In this study, we propose a two-crack based complementary nanoelectromechanical (CNEM) switch operating as a CMOS inverter. Remarkably, complementary switching, which spontaneously occurs once cracks are induced, provides a simple way to construct RC.

II. Experiments

The ferroelectric substrate we used was 500-μm thick (001)-oriented $[Pb(Mg_{1/3}Nb_{2/3})O_3]0.7$-$[PbTiO_3]0.3$ (PMN−PT) single crystal. A 40-nm MnPt intermetallic alloy film was sputtered from a $Mn_{50}Pt_{50}$ metallic target using a magnetron sputtering system at room temperature. Then, the MnPt film was processed into two separate rectangular areas with a size of 50×100 μm^2 and a gap width of 6 μm by using photolithography and argon ion milling. Thereafter, a Keithley 2410 source meter was used to apply a triangular cyclic control voltage with an amplitude of 30 V and a period of 120 s between these two MnPt areas to induce cracks (for details, see ref. [19]). Subsequently, the same control voltage was used to manipulate the switching of cracks. For the electrical measurements, Keithley 2400 and 2450 source meters were used to apply a constant voltage of 1 mV across

Manuscript received January 27, 2020; revised March 22, 2020; accepted March 24, 2020. Date of publication March 27, 2020; date of current version April 24, 2020. This work was supported in part by the National Natural Science Foundation of China under Grant 61674062, Grant 61904060, and Grant 61821003, in part by the Fundamental Research Funds for the Central Universities under Grant HUST: 2018KFYXKJC019, and in part by the Research Project of Wuhan Science and Technology Bureau under Grant 2019010701011394. The work of Zhe Guo was supported by the China Postdoctoral Science Foundation. The review of this letter was arranged by Editor D. G. Senesky. *(Corresponding author: Long You.)*

The authors are with the School of Optical and Electronic Information, Huazhong University of Science and Technology, Wuhan 430074, China (e-mail: lyou@hust.edu.cn).

Color versions of one or more of the figures in this letter are available online at http://ieeexplore.ieee.org.

Digital Object Identifier 10.1109/LED.2020.2983735

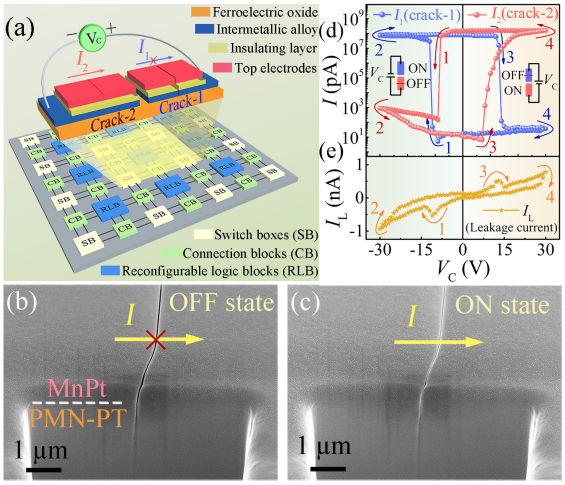

Fig. 1. (a) Schematic of the crack-based CNEM switches. The device comprises a ferroelectric oxide and an intermetallic alloy thin film grown thereon. For further actual application, a multilayer stack with an inserted insulating layer could be used, replacing the single layer film. The control voltage V_C was applied on two separate rectangular patterns such that the complementary switching of two cracks occurs. The opening of one crack is always accompanied by the closing of the other one. This property can be employed to construct programmable routings and logic blocks of RC. The cross-section SEM images of crack-1 with (b) open state and (c) closed state based on the PMN-PT/MnPt heterostructure. The hole is fabricated via FIB etching [19]. (d) *I–V* characteristics of the crack-based CNEM switches. (e) Corresponding leakage current (I_L) in the PMN-PT substrate. The arrows and numbers in (d) and (e) indicate the field-sweeping sequence.

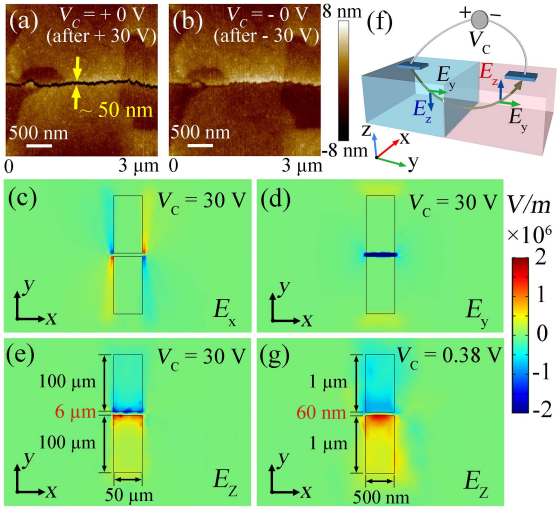

Fig. 2. (a) and (b) AFM images ($3 \times 3\ \mu m^2$) of one crack after scanning V_C from +30 to 0 V and from −30 to 0 V, respectively. (c)-(e) Top-view distributions of x-, y- and z-components of electric fields via COMSOL Multiphysics simulation. (f) Schematic of the electric field decomposition. (g) Z-component of electric field distribution with a gap width of 60 nm.

the two cracks and measured the channel currents I_1 and I_2, respectively.

III. Results and Discussion

As schematically illustrated in Fig. 1(a), the device consists of two main parts: (1) switchable cracks induced by ferroelectric domain switching, (2) the current path in metallic films controlled by the states of extended cracks. Fig. 1(b) clearly demonstrates the spatial structure based on a PMN-PT/MnPt heterostructure, in which the crack propagates from PMN-PT into the MnPt film. In our case, the writing operation is implemented by applying the control voltage V_C onto the ferroelectric oxide. Specifically, one of the two cracks (crack-1 or crack-2) is always at OFF state and the other is ON. The polarity of V_C determines these states. The readout operation is performed by detecting the states of cracks using a small constant voltage, thus achieving a non-destructive process. Fig. 1(b) and 1(c) clearly illustrate the open and closed state of one crack. The air gap at OFF state can entirely block the current in the film while the area metallic contacts recover back to its ON state.

In actual experiment, an MnPt intermetallic alloy thin film was selected owing to its moderate mechanical property [18]. Fig. 1(d) shows the electrical performance with readout operating at 1 mV. The initial states, i.e., $I_1 \approx 10$ pA and $I_2 \approx 150\ \mu$A when $V_C = 0$ V, correspond to a high-resistance state (OFF) of crack-1and low-resistance state (ON) of crack-2. The negative V_C with an average magnitude of 15 V sharply switched the crack states whereas the symmetrical positive V_C recovered the cracks to the initial states. The demonstrated square non-volatile switching loop could be associated with the 109° domain switching in PMN-PT [20]. The ferroelectric leakage current (I_L) in PMN-PT (Fig. 1e) indicated that the peaks of I_L exactly corresponded to the crack switching field, which further confirmed the correlation between the domain switching and switchable cracks [18], [19].

Furthermore, the surface morphology details of the crack were imaged via atomic force microscopy (AFM). Given that V_C was swept from +30 to 0 V, the crack remained in open state with a width of ~50 nm (Fig. 2a) and it had a close contact after applying $V_C = -30$ V (Fig. 2b). Next, we discuss the mechanism for the complementary switching of cracks. As reported previously [18], [19], crack formation in such a heterostructure was induced by the local micron-scale strain at the domain boundaries originating from the electrically switchable ferroelectric domains and defect-pinned domains. Therefore, we analyzed the electric field distributions in our device, which mainly determine the domain switching process.

We conducted simulations of x-, y- and z-components of electric fields (Ex, Ey and Ez) using the COMSOL software. Fig. 2(e) clearly shows the exactly opposite distribution of Ez in the two studied areas. In contrast, Ex (Fig. 2c) is nearly zero owing to the symmetry, and Ey (Fig. 2d) does not vary in the two areas, thereby preventing its contribution to the complementary switching. From the schematic of the electric field decomposition shown in Fig. 2(f), we can easily conclude that Ez is opposite and Ey is always the same at a symmetrical position. This agrees with the simulated results. Accordingly, the complementary switching of cracks is mainly determined by the Ez distribution. Considering further dimensional scaling, V_C will be drastically reduced with the decrease in gap width between two separated film areas, given that switching is dominated by electric field rather than by the voltage magnitude. For example, when the gap width is reduced to 60 nm, the required voltage to obtain similar E_Z distribution is significantly reduced to 0.38 V, as shown in Fig. 2(g).

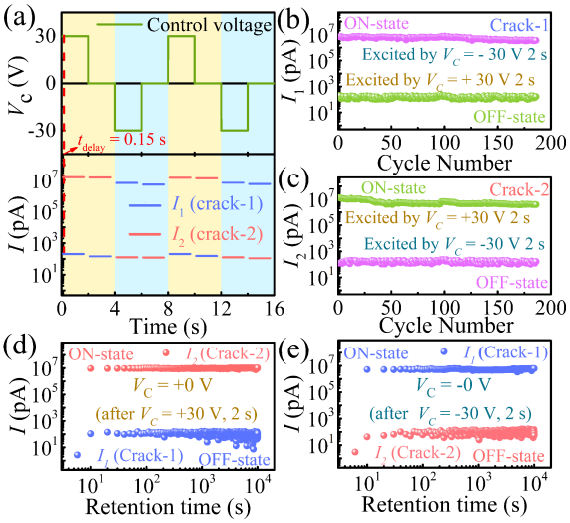

Fig. 3. (a) The upper plot shows the applied voltage signals whereas the lower one illustrates the measured currents I_1 and I_2. The data were collected both when the voltage was applied and removed. (b) and (c) The repeatability test for the opening and closing of the cracks via voltage pulses, respectively. (d) and (e) Data retention performances.

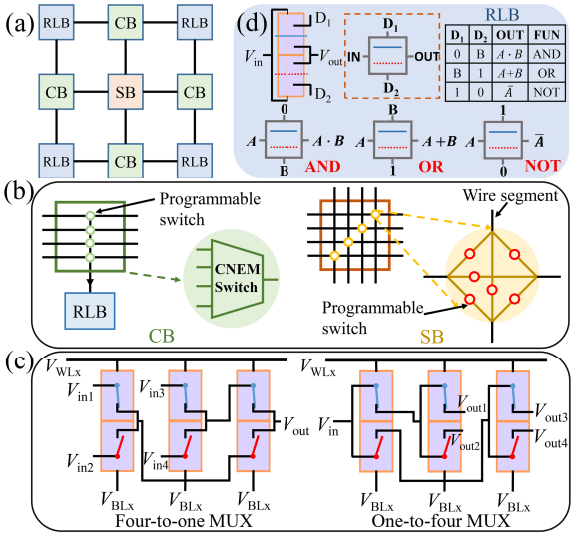

Fig. 4. Block diagrams of the proposed RC based on CNEM switches. (a) Schematic of a generic FPGA. (b) Internal structures of programmable CB and SB. (c) Four-to-one MUX (left panel) and one-to-four MUX (right panel) based on CNEM switches. (d) RLB based on CNEM switches.

We also investigated the switching performance under voltage pulses. An alternating ±30 V voltage signal with a pulse time of 2 s (Fig. 3a) was applied. The current I_1 and I_2 were measured with a delay time of 0.15 s after the voltage pulse was applied and removed. From the obtained results, we concluded that the positive voltage pulse led to low values of I_1 (represented by blue line) and the high values of I_2 (indicated by red line), while the negative voltage induced high values of I_1 and low values of I_2, demonstrating complementary switching. Remarkably, when the pulse was removed, the values of I_1 and I_2 remained unchanged, illustrating a stable nonvolatile control of these two cracks.

Subsequently, we performed the repeatability test. The data were collected during the application of the voltage. As shown in Fig. 3(b) and 3(c), the reversible opening and closing of the cracks could be cycled for several hundred times and the current ON/OFF ratio is maintained around 10^4. Note that the closing state of cracks would degrade due to the contact contamination and the uneven contact surface. It is expected that the endurance could be largely increased by using the contact material with high robustness to the surface contamination and the ferroelectric layer with a regular domain structure [19]. In addition, after applying a single voltage pulse, the retention data for two cracks were collected within 10^4 s and the states remained unchanged all the time, as shown in Fig. 3(d) and Fig. 3(e), respectively.

Next, we discuss the implementation of RC based on our crack-based CNEM switches. As a typical enabler of RC, conventional island-style FPGA architectures [21] mainly comprise reconfigurable logic blocks (RLB), connection boxes (CB) and switch boxes (SB) in which the CBs connect adjacent RLBs with each other and interface the LBs to the channels, as shown in Fig. 4(a).

From the above results and discussions, it was demonstrated that our CNEM switches are appropriate for implementing energy-efficient CB and SB. This plays a key role in dynamic operating of FPGAs. Fig. 4(b) shows the internal structure of programmable CBs and SBs, which consist of numerous multiplexers (MUXs) [7], [12]. The four-to-one and one-to-four MUX cases based on our CNEM switches are shown in Fig. 4(c). In these cases, smaller time delay compared with the CMOS-based counterpart could be achieved owing to the simple signal passing paths without additional selecting transistors [7]. Moreover, the low ON-resistance can significantly reduce the dynamic power. Particularly, the nonvolatile control of crack states enables the data signal paths to be maintained without any control voltage.

For the RLB module, our crack-based CNEM switches could achieve a variety of logic functions within a limited number of devices, providing a higher integration density for RC. For example, as shown in Fig. 4(d), basic logic functions such as AND, OR and NOT can be implemented with a single device by programming the data signals D_1 and D_2. From the truth table, it can be concluded that such a device can achieve the logic function as follows: $OUT = \overline{IN} \cdot D_1 + IN \cdot D_2$. Note that for isolating the output from the input signals, an insulating layer should be integrated into the device structure.

IV. Conclusion

In summary, RC implemented by the crack-based CNEM switches is proposed in this letter. Programmable interconnections based on complementary switching of cracks were demonstrated. Low dynamic and static power consumption were obtained owing to the low ON-resistance and quasi-zero OFF-state leakage current. In addition, the proposed technology consumes less device numbers than the conventional realization of RC, offering potential for high integration density. We believe that the proposed technology provides a new way for RC and promote the 'More than Moore' paradigm.

REFERENCES

[1] K. Bondalapati and V. K. Prasanna, "Reconfigurable computing systems," *Proc. IEEE*, vol. 90, no. 7, pp. 1201–1217, Jul. 2002, doi: 10.1109/JPROC.2002.801446.

[2] A. DeHon, "Fundamental underpinnings of reconfigurable computing architectures," *Proc. IEEE*, vol. 103, no. 3, pp. 355–378, Mar. 2015, doi: 10.1109/JPROC.2014.2387696.

[3] R. Tessier, K. Pocek, and A. DeHon, "Reconfigurable computing architectures," *Proc. IEEE*, vol. 103, no. 3, pp. 332–354, Mar. 2015, doi: 10.1109/JPROC.2014.2386883.

[4] I. Kuon, R. Tessier, and J. Rose, "FPGA architecture: Survey and challenges," *Found. Trends Electron. Design Autom.*, vol. 2, no. 2, pp. 135–253, Apr. 2008, doi: 10.1561/1000000005.

[5] A. B. Kahng, "Scaling: More than Moore's law," *IEEE Des. Test. IEEE Des. Test. Comput.*, vol. 27, no. 3, pp. 86–87, May 2010, doi: 10.1109/MDT.2010.71.

[6] Y.-B. Kim, "Challenges for nanoscale MOSFETs and emerging nanoelectronics," *Trans. Electr. Electron. Mater.*, vol. 11, no. 3, pp. 93–105, Jun. 2010, doi: 10.4313/TEEM.2010.11.3.093.

[7] Y. Jun Kim and W. Young Choi, "Nonvolatile nanoelectromechanical memory switches for low-power and high-speed field-programmable gate arrays," *IEEE Trans. Electron Devices*, vol. 62, no. 2, pp. 673–679, Feb. 2015, doi: 10.1109/TED.2014.2380992.

[8] T. Skotnicki, J. A. Hutchby, T. King, H.-S.-P. Wong, and F. Boeuf, "The end of CMOS scaling," *IEEE Circuits Devices Mag.*, vol. 21, no. 1, pp. 16–26, Jan. 2005, doi: 10.1109/MCD.2005.1388765.

[9] H. Dery, P. Dalal, Ł. Cywiński, and L. J. Sham, "Spin-based logic in semiconductors for reconfigurable large-scale circuits," *Nature*, vol. 447, no. 7144, pp. 573–576, May 2007, doi: 10.1038/nature05833.

[10] W. Y. Kim, H.-D. Kim, T.-T. Kim, H.-S. Park, K. Lee, H. J. Choi, S. H. Lee, J. Son, N. Park, and B. Min, "Graphene–ferroelectric metadevices for nonvolatile memory and reconfigurable logic-gate operations," *Nature Commun.*, vol. 7, no. 1, p. 10429, Apr. 2016, doi: 10.1038/ncomms10429.

[11] C. Qian, A. Peschot, B. Osoba, Z. A. Ye, and T.-J.-K. Liu, "Sub-100 mV computing with electro-mechanical relays," *IEEE Trans. Electron Devices*, vol. 64, no. 3, pp. 1323–1329, Mar. 2017, doi: 10.1109/TED.2017.2657554.

[12] T. Qin, S. J. Bleiker, S. Rana, F. Niklaus, and D. Pamunuwa, "Performance analysis of nanoelectromechanical relay-based field-programmable gate arrays," *IEEE Access*, vol. 6, pp. 15997–16009, Mar. 2018, doi: 10.1109/ACCESS.2018.2816781.

[13] V. Garcia, S. Fusil, K. Bouzehouane, S. Enouz-Vedrenne, N. D. Mathur, A. Barthélémy, and M. Bibes, "Giant tunnel electroresistance for non-destructive readout of ferroelectric states," *Nature*, vol. 460, no. 7251, pp. 81–84, Jul. 2009, doi: 10.1038/nature08128.

[14] J.-W. Han, J.-H. Ahn, M.-W. Kim, J. O. Lee, J.-B. Yoon, and Y.-K. Choi, "Nanowire mechanical switch with a built-in diode," *Small*, vol. 6, no. 11, pp. 1197–1200, Jun. 2010, doi: 10.1002/smll.201000170.

[15] J. O. Lee, Y.-H. Song, M.-W. Kim, M.-H. Kang, J.-S. Oh, H.-H. Yang, and J.-B. Yoon, "A sub-1-volt nanoelectromechanical switching device," *Nature Nanotechnol.*, vol. 8, no. 1, pp. 36–40, Jan. 2013, doi: 10.1038/NNANO.2012.208.

[16] O. Y. Loh and H. D. Espinosa, "Nanoelectromechanical contact switches," *Nature Nanotechnol.*, vol. 7, no. 5, pp. 283–295, May 2012, doi: 10.1038/NNANO.2012.40.

[17] J. Fujiki, N. Xu, L. Hutin, I.-R. Chen, C. Qian, and T.-J.-K. Liu, "Microelectromechanical relay and logic circuit design for zero crowbar current," *IEEE Trans. Electron Devices*, vol. 61, no. 9, pp. 3296–3302, Sep. 2014, doi: 10.1109/TED.2014.2336855.

[18] Z. Q. Liu, J. H. Liu, M. D. Biegalski, J.-M. Hu, S. L. Shang, Y. Ji, J. M. Wang, S. L. Hsu, A. T. Wong, M. J. Cordill, B. Gludovatz, C. Marker, H. Yan, Z. X. Feng, L. You, M. W. Lin, T. Z. Ward, Z. K. Liu, C. B. Jiang, L. Q. Chen, R. O. Ritchie, H. M. Christen, and R. Ramesh, "Electrically reversible cracks in an intermetallic film controlled by an electric field," *Nature Commun.*, vol. 9, no. 1, p. 41, Dec. 2018, doi: 10.1038/s41467-017-02454-8.

[19] Q. Luo, Z. Guo, H. Huang, Q. Zou, X. Jiang, S. Zhang, H. Wang, M. Song, B. Zhang, H. Chen, H. Gu, G. Han, X. Yang, X. Zou, K.-Y. Wang, Z. Liu, J. Hong, R. Ramesh, and L. You, "Nanoelectromechanical switches by controlled switchable cracking," *IEEE Electron Device Lett.*, vol. 40, no. 7, pp. 1209–1212, Jul. 2019, doi: 10.1109/LED.2019.2917924.

[20] S. Zhang, Y. G. Zhao, P. S. Li, J. J. Yang, S. Rizwan, J. X. Zhang, J. Seidel, T. L. Qu, Y. J. Yang, Z. L. Luo, Q. He, T. Zou, Q. P. Chen, J. W. Wang, L. F. Yang, Y. Sun, Y. Z. Wu, X. Xiao, X. F. Jin, J. Huang, C. Gao, X. F. Han, and R. Ramesh, "Electric-field control of magnetism in $Co_{40}Fe_{40}B_{20}$/(1-x)Pb($Mg_{1/3}Nb_{2/3}$)O_3-x$PbTiO_3$ multiferroic heterostructures with different ferroelectric phases," *Phys. Rev. Lett.*, vol. 108, no. 13, Mar. 2012, Art. no. 137203, doi: 10.1103/PhysRevLett.108.137203.

[21] Z. Zhang, Y. Y. Liauw, C. Chen, and S. S. Wong, "Monolithic 3-D FPGAs," *Proc. IEEE*, vol. 103, no. 7, pp. 1197–1210, Jul. 2015, doi: 10.1109/JPROC.2015.2433954.